Audio Engineering Society

Convention Paper 6954

Presented at the 121st Convention
2006 October 5–8 San Francisco, CA, USA

Spring Reverb Emulation Using Dispersive Allpass Filters in a Waveguide Structure

Jonathan S. Abel[1,2], David P. Berners[1,2], Sean Costello[3], Julius O. Smith III[2]

[1] *Universal Audio, Inc., Santa Cruz, CA, 95060, USA*

[2] *CCRMA, Stanford University, Stanford, CA, 94305, USA*

[3] *Analog Devices, San Jose, CA, 95110, USA*

Correspondence should be addressed to Jonathan S. Abel (`abel@uaudio.com`)

ABSTRACT

Wave propagation along springs in a spring reverberator is studied, and digital emulations of several popular spring reverberator models are presented. Measurements on a number of springs reveal several dispersive propagation modes and evidence of coupling between them. The torsional mode typically used by spring reverberators is seen to be highly dispersive, giving the spring its characteristic sound. Spring reverberators often have several springs operating in parallel, and the emulations presented here use a set of parallel waveguide structures, one for each spring element. The waveguides explicitly compute the left-going and right-going torsional waves, including dispersion, propagation and reflection effects. Scattering from spring imperfections and from the rings coupling counter-wound springs are modeled via waveguide scattering junctions.

1. INTRODUCTION

Helical springs support a number of transmission modes for mechanical vibrations at audio frequencies, including transverse, longitudinal and torsional modes, as illustrated in Figure 1. Typically, springs are driven near one end. Depending upon the direction of the driving force, particular modes or combinations of modes will be excited on the spring. A delayed signal will then appear at the other end, with the amount of delay being determined by the wave propagation speed for the mode(s) excited.

As early as the 1920s, springs were used to delay audio signals for telephone applications such as echo cancellation [1]. Helical springs have long been used for artificial reverberation [3], and are still a popular choice for guitar amp reverberators. The propagation modes within springs are strongly dispersive, giving spring reverberators a distinctive sound.

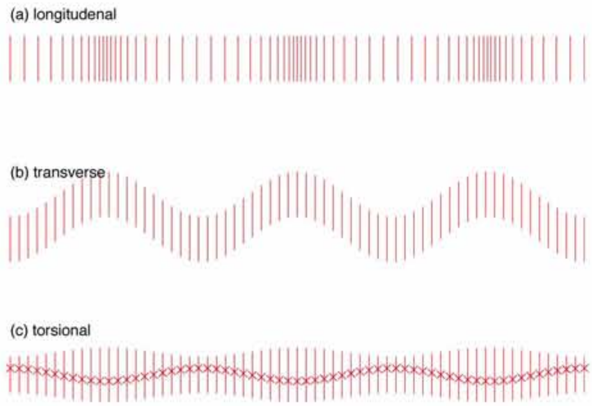

Fig. 1: *Spring Propagation Modes. Transverse (a), longitudinal (b) and torsional (c) spring propagation modes are shown.*

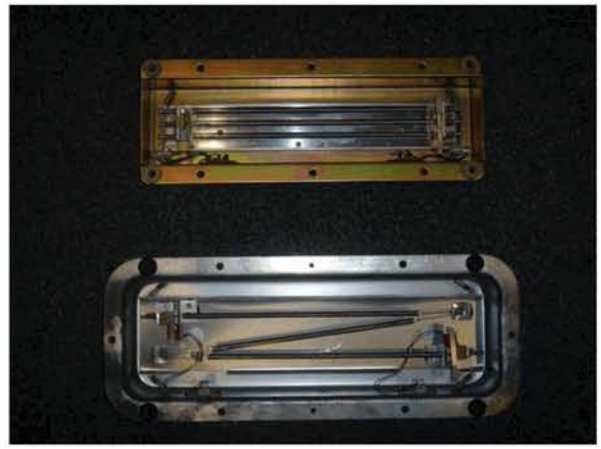

Fig. 2: *Accutronics Type 8 Spring Tank (top); Single Spring 'Folded' into a Compact Space (bottom).*

In the late 1930s, Hammond configured springs so that propagating waves would be reflected back and forth, creating a series of echoes reminiscent of reverberation [2]. Modern-day spring reverberators take a very similar approach, often using two or three springs of different lengths in parallel to increase echo density, and driving the springs torsionally to minimize susceptibility to mechanical shock [3, 4]. In this paper, spring wave-propagation mechanisms are explored and used to develop discrete-time emulations of several popular spring reverberators.

In §2 it is argued that springs are approximately linear and time invariant at typical operating levels, and, as a result, may be studied by considering their impulse response. Measurements are presented showing that the torsional mode used by modern springs is strongly dispersive, and that little energy propagates above a cutoff frequency.

A discrete-time spring model is presented in §3. The model employs a set of parallel waveguide structures, one for each spring element. This model is appropriate for spring reverberators containing spring elements arranged in parallel, with no coupling between springs, as seen in Figure 2. Reverberators occasionally have spring elements comprised of spring segments connected in series, as seen in Figure 2; such arrangements are emulated using waveguides with scattering junctions between modeled spring segments. Emulation results are given in §4, with the waveguide model tuned to match an Accutronics Type 8 spring tank and a Sansui RA-700 spring reverberator.

2. SPRING PROPAGATION

The spring reverberators studied here consist of several (usually two or three) independent spring elements, operating in parallel. Swept sinusoid measurements on a variety of such reverberators show them to be approximately linear and time invariant at typical operating levels. Further, measurement shows that there is typically little, if any, interaction between spring elements, and the elements may thus be analyzed and modeled separately. The individual element models can be created based solely on impulse-response data, because of the linearity of the system.

As shown in Figure 3, the springs studied here are stretched between two supports, and have magnetic beads attached to their ends. The bead at the driver end is rotated according to the input, and the resulting torsional wave propagates along the length of the spring. When the wave reaches the pick-up end of the spring, it will twist against the rigid support and be reflected back along the spring toward the driver. A pick-up detecting bead rotation will therefore see a series of echoes in response to input signals.

Since the driver and pick-up are at opposite ends of the spring, echo arrivals are expected at odd integer

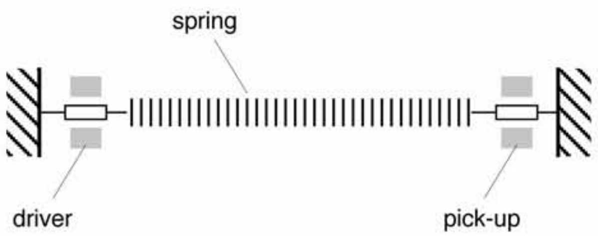

Fig. 3: *Helical Spring Element.*

multiples of the travel time between driver and pick-up. Successive echoes will be reduced in amplitude, as signal energy is lost to damping with each end reflection and to heat as the coils wind and unwind with the passing wave.

Impulse response measurements on individual spring elements show a damped series of echoes with the expected timing. However, the individual echoes are noticeably smeared over time, as seen in the example of Fig. 4. Studying the spectrogram of the first few arrivals, as in Figure 5, we see that low-frequency signals propagate faster than high-frequency signals, turning each arrival into a chirp.

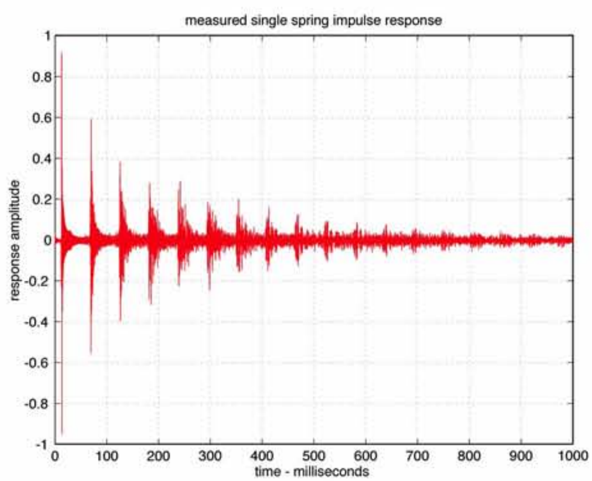

Fig. 4: *Accutronics Type 8 Spring Element Impulse Response.*

Several other features of the spring-element spectrogram are of note. It seems that little energy propagates above a cutoff frequency (around 4 kHz

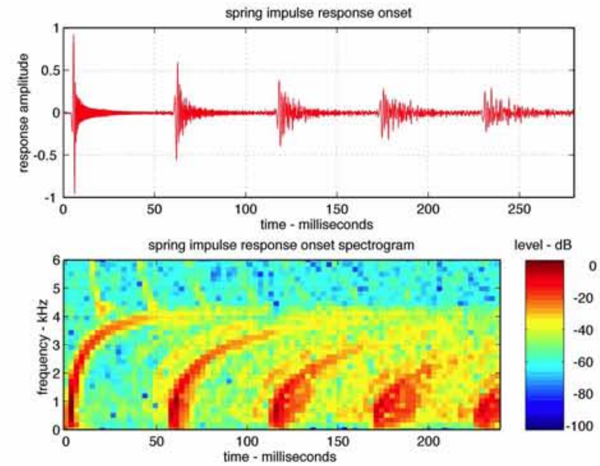

Fig. 5: *Accutronics Type 8 Impulse Response Onset and Spectrogram*

for many of the springs tried), contributing to the spring's equalization. This appears to be related to the wavelength of signals traveling on the spring [3, pg. 288]: torsional waves spanning just a few coils take on a very small group velocity.

Above the cutoff, there is another propagation mode having a speed several times that of the mode propagating below the cutoff. It appears in the output with fairly low amplitude, and is weakly dispersive, propagating high frequencies faster than low frequencies. Since it shares the cutoff frequency with the main torsional mode, this mode could be a torsional bending mode of the spring.

Some spring elements comprise a pair of counter-wound springs connected in series. The idea is that torsional waves will wind the spring, changing the coil spacing, and thereby creating longitudinal waves. Longitudinal and torsional waves propagate at slightly different speeds, and couple to each other continuously along the spring. By winding the spring in one direction for half its length, and the other direction for the remainder of its length, this effect is reduced. When doing this, however, there may be scattering from the junction between the lengths of spring, creating additional reflections.

In a single length of spring, for example as seen in Figure 5, the impulse response spectrogram has arrivals which, at any given frequency, become increasingly smeared over time. Eventually the arrivals are sufficiently smeared that they give the impulse response a noise-like 'wash' rather than the repeated chirp heard for much of the impulse response.

Referring to Figure 5, note that successive reflections have opposite signs.

3. WAVEGUIDE MODEL

The spring reverberator emulation presented here consists of a set of parallel waveguide structures [5], one for each spring element. Each element model consists of a waveguide propagating left-going and right-going torsional waves, with the propagation dispersion and attenuation commuted to the waveguide ends, as shown in Figure 6.

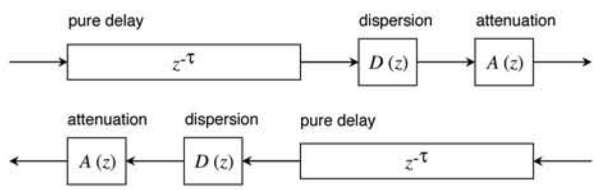

Fig. 6: *Waveguide Section. Left-going and right-going waves are separately processed via pure delay elements and commuted dispersion and propagation loss filters.*

The needed dispersion is estimated by examining successive arrivals in the spring element impulse response. A recently developed method for dispersion filter design [6, 7] was used to fit an allpass filter to the measured time delay as a function of frequency. The waveguide is terminated by reflection filters, which, when combined with the attenuation filters, are designed to account for the attenuation seen in successive arrivals. Finally, scattering junctions are inserted into the waveguides to account for spring imperfections and to model the scattering between counter-wound springs. Figure 7 shows the model for a set of counter-wound springs with scattering occurring at the spring end-points and also at the ring connecting the counter-wound segments. Scattering junctions can also be added to model reflections caused by localized irregularities in the springs, including changes in cross-sectional area or nicks/scratches/cuts. In Figure 7, each block labeled "waveguide section" corresponds to the bi-directional series connection of pure delay, dispersion filtering, and attenuation filtering shown in Figure 6.

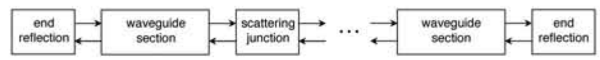

Fig. 7: *Waveguide Spring Element Model. Each spring element is modeled using a set of waveguide sections, connected via scattering junctions, and terminated at the spring ends.*

The model of Figure 7 can be extended to account for the above-cutoff propagation mode mentioned in §2. This would be accomplished by adding a second, parallel waveguide, with a different (shortened) delay length corresponding to the increased group velocity of the mode. Because of the low amplitudes associated with this mode, it has been neglected.

Figure 8 shows a detail of the scattering junctions of Figure 7. Since losses within the waveguide have already been accounted for by the filters within Figure 6, the scattering junctions are *lossless, i.e.,* $R^2 + T^2 = 1$ at every frequency. If the spring terminations are relatively stiff (lossless), the termination reflection filter $M(z)$ will tend towards an all-pass filter.

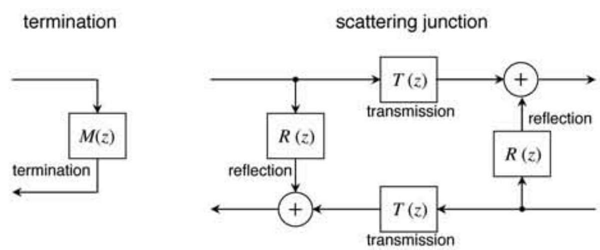

Fig. 8: *Scattering Junction and Spring Element Termination.*

4. EXAMPLE EMULATION

Accutronics Type 8 (shown in Figure 2) and Sansui RA-700 spring reverberators were modeled. Figure 9 shows detailed time-plots of the first reflections of a spring element from one of the units. As can be seen, the energy is localized near $t = 0$ in the top trace, while the lower traces have impulse responses with a

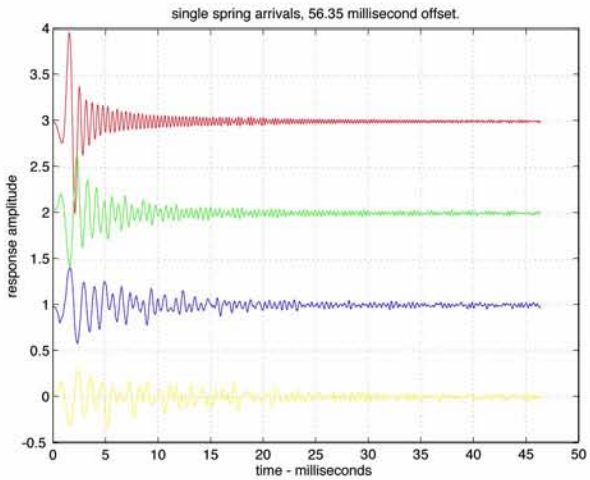

Fig. 9: *Spring Element Arrivals.*

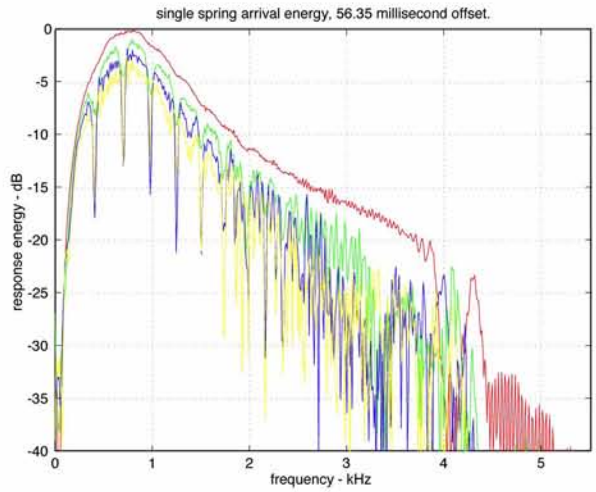

Fig. 10: *Arrival Transform Magnitudes.*

longer duration. The total amount of energy in the lower plots is also reduced.

Round-trip filtering due to losses in the spring and scattering accounts for the differences between the traces of Figure 9. Dispersion in the spring causes the lengthening of successive reflections. Frequency-dependent losses also change the relative shapes of the reflections. Figure 10 shows magnitude spectral plots for the reflections. Doing a pointwise division of the spectral transforms results in the *transform magnitude ratio* plots of Figure 11. By dividing the transform magnitudes of successive reflections, the filtering impressed on the signal during one round trip through the spring can be calculated. The N spectra of Figure 10 therefore can be used to produce $N-1$ spectral ratios of Figure 11. A smoothed filter, designed to fit the data of Figure 11, can be inserted into the waveguide model as $A(z)$ in Figure 6. Since there are two instances of filter $A(z)$ in one round trip through the spring, the filter must be fit to the square-root of the data in Figure 11.

The remaining behavior which needs to be modeled is the dispersion associated with the spring. Figure 12 shows the group delay associated with one round trip through the spring. This plot was generated by finding the group delay associated with each of the reflections of Figure 9, with the reflections treated as impulse responses. The group delays for the reflections are superimposed, after scaling by $1, 1/3, 1/5, \ldots$ to account for the total number of round trips completed by each reflection. These plots show the total (scaled) amount of group delay incurred by one round trip through the spring. An allpass filter matching one half of this group delay can be inserted as $D(z)$ in Figure 6. Figure 13 shows the desired group delay, superimposed with the group delay of the allpass filter used to approximate the delay. Note that the delay plotted is mainly the dispersive component of the spring delay, with much of the bulk delay removed and implemented as the delay line in Figure 6. Also note that the filter $A(z)$ will have some group delay associated with it, and although this delay is small, it has been subtracted from the measured round-trip dispersive delay to find the desired group delay modeled by $D(z)$.

Figure 14 shows a spectrogram of the Accutronics Type 8 impulse response, along with the impulse response of the model. The three springs in the unit produce reflections with similar delays, which spread out and become distinct as more round trips are completed. Notice that for both the measured response and the model, low-frequency energy precedes high-frequency energy in each reflection

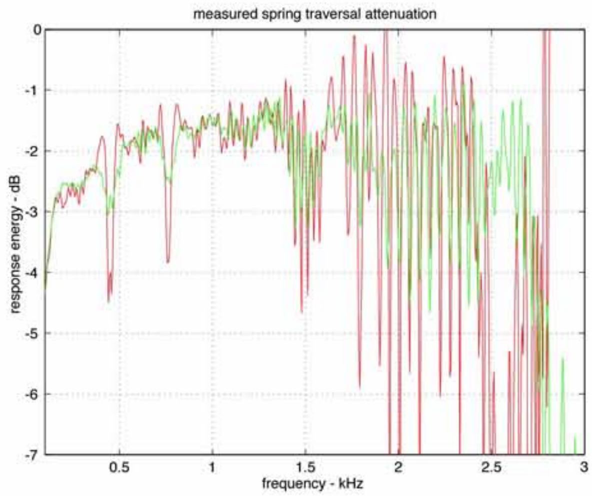

Fig. 11: *Successive Arrival Transform Magnitude Ratios.*

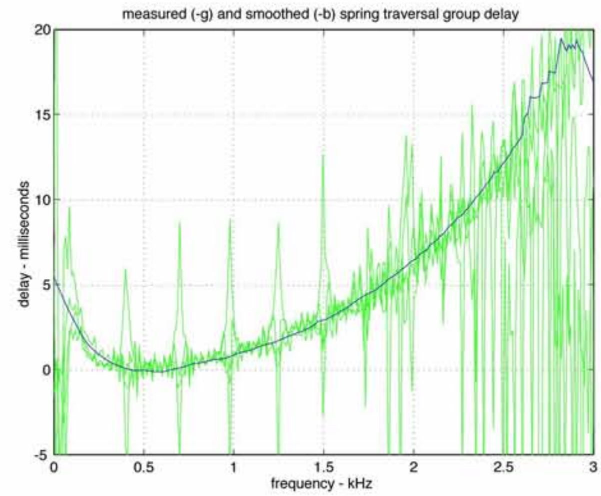

Fig. 12: *Spring Element Arrival Dispersive Group Delay*

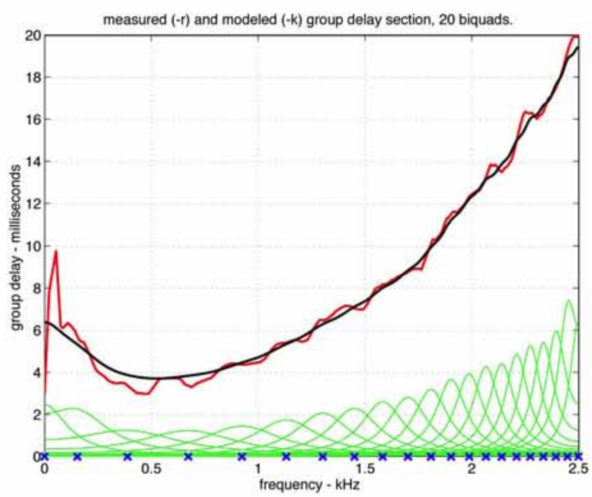

Fig. 13: *Example Measured and Modeled Dispersive Group Delay*

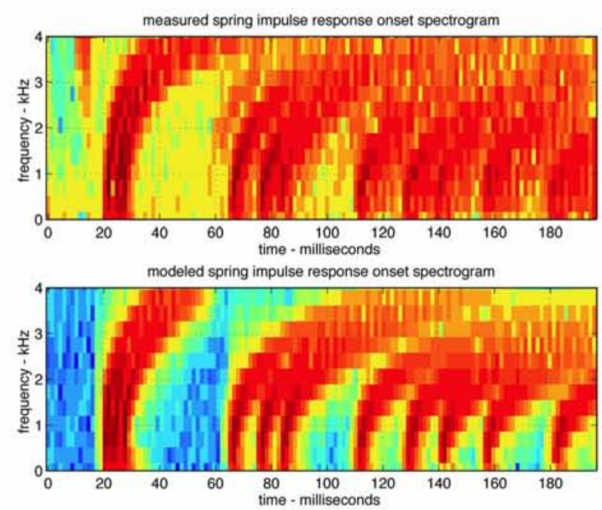

Fig. 14: *Measured and Modeled Accutronics Type 8 Impulse Response Spectrograms.*

because of the dispersion, and the smearing of energy accumulates as time progresses. Listening tests show good perceptual agreement between the modeled springs and emulations.

5. SUMMARY

A computationally efficient model has been presented which captures the linear, time-invariant portion of the response of a spring reverberator. Methods have been shown for fitting the elements of the model to data which can be easily collected from the unit to be emulated. Examples have been presented which outline the process, showing good agreement between the model and the system being modeled.

6. ACKNOWLEDGMENT

The authors would like to thank Rolf Bader of the University of Hamburg for many valuable discussions on this and related topics.

7. REFERENCES

[1] R. L. Wegel, "Wave Transmission Device," US Patent No. 1,852,795, April 5, 1932.

[2] Laurens Hammond, "Electrical Musical Instrument," US Patent No. 2,230,836, February 4, 1941.

[3] H. E. Meinema, H. A. Johnson and W. C. Laube, Jr., "A New Reverberation Device for High Fidelity Systems," *Journal of the Audio Engineering Society*, vol. 9, no. 4, October, 1961.

[4] Alan C. Young, "Artificial Reverberation Unit," US Patent No. 3,106,610, October 8, 1963.

[5] Julius O. Smith, *Physical Audio Signal Processing* http://ccrma.stanford.edu/ jos/pasp/, Aug. 2006, online book.

[6] J. S. Abel, J. O. Smith, and J. Bensa, "An allpass filter design method with application to piano string synthesis," in *Acoust. Soc. of Amer.*, Program of the 149th Meeting, Vancouver, Canada, May 2005.

[7] J. S. Abel and J. O. Smith, "Robust design of very high-order dispersive allpass filters," to appear in *Proc. of the 9th Int. Conference on Digital Audio Effects (DAFx'06)*, Montreal, Canada, September 18–20, 2006.